31

POLYMER NANOCOMPOSITES

OCTAVIO MANERO AND ANTONIO SANCHEZ-SOLIS

31.1 INTRODUCTION

Polymeric nanocomposites are a class of relatively new materials with ample potential applications. Products with commercial applications appeared during the last decade [1], and much industrial and academic interest has been created. Reports on the manufacture of nanocomposites include those made with polyamides [2–5], polyolefins [6–9], polystyrene (PS) and PS copolymers [10, 11], ethylene vinyl alcohol [12–15], acrylics [16–18], polyesters [19, 20], polycarbonate [21, 22], liquid crystalline polymers [8, 23–25], fluoropolymers [26–28], thermoset resins [29–31], polyurethanes [32–37], ethylene–propylene oxide [38], vinyl carbazole [39, 40], polydiacethylene [41], and polyimides (PIs) [42], among others.

Generally, polymer nanocomposites can be obtained through two routes: the first one is the polymerization of monomers in contact with the exfoliated clay and the second one uses existing transformation processes to produce nanocomposites, for example, by a reactive extrusion. There are, however, problems present due to the lack of affinity of the clay–polymer system because of the hydrophilic character of the particles. It is then necessary to treat the clay chemically to increase its affinity with the polymer matrix. This constitutes another whole area of research in the nanocomposites production.

The mixing of the nanoparticle with the polymer requires an intercalation process of the macromolecule into the clay galleries gap. This is a diffusion-controlled process that requires long contact times between the polymer and the clay under the pressure produced inside the extruder. The intercalation process leads to the exfoliation of the clay. However, low screw speeds and long residence times in the extruder may cause polymer degradation. To avoid such problem that would enable complete clay exfoliation, it would be necessary to change the screw configuration or to consider the chemical modification of the clay. Moreover, clay exfoliation is not a sufficient condition to obtain optimum system performance. The problem of compatibility of the clay–polymer matrix is an outstanding one, and the thermodynamic processes involved in the synthesis of these materials [43, 44] constitute areas that are currently under investigation.

The macroscopic effects of the integration of nanoparticles into the polymer matrix are quite remarkable. For example, the barrier properties of the new systems are enhanced since the diffusion of gas molecules through the material is largely retarded. A lower permeability of O_2 is obtained without substantially modifying the production method of films, containers, bottles, etc. Oxygen permeability decreases drastically with nanoparticle concentration.

This chapter covers fundamental and applied research on polyester/clay nanocomposites (Section 31.2), which includes polyethylene terephthalate (PET), blends of PET and poly(ethylene 2,6-naphthalene dicarboxylate) (PEN), and unsaturated polyester resins. Section 31.3 deals with polyethylene (PE) and polypropylene (PP)–montmorillonite (MMT) nanocomposites, including blends of low density polyethylene (LDPE), linear low density polyethylene (LLDPE), and high density polyethylene (HDPE). Section 31.4 analyzes the fire-retardant properties of nanocomposites made of high impact polystyrene (HIPS), layered clays, and nonhalogenated additives. Section 31.5 discusses the conductive properties of blends of PET/PMMA (poly (methyl methacrylate)) and PET/HDPE combined with several types of carbon

Handbook of Polymer Synthesis, Characterization, and Processing, First Edition. Edited by Enrique Saldívar-Guerra and Eduardo Vivaldo-Lima.

black (CB). The synthesis and potential applications of barium sulfate particles with various morphologies (fibers, spherical) are discussed in Section 31.6, and finally, in Section 31.7 the new nanocomposites of graphene are briefly exposed.

31.2 POLYESTER/CLAY NANOCOMPOSITES

31.2.1 PET–Clay Nanocomposites

The processing of polymeric nanocomposites based on PET and a clay, MMT, was analyzed elsewhere [45]. The clay was chemically modified with a quaternary ammonium salt, and this was subsequently incorporated into the polymer using maleic anhydride (MAH) and pentaerythritol (PENTA) as compatibilizing agents.

An interesting observation is the reported decrease in melt viscosity of organo-clay composites, with respect to the matrix viscosity [46, 47]. Results reveal that PET nanocomposites behave quite differently in shear as opposed to elongation.

Nanocomposites of MMT polymer can be obtained by direct polymer melt intercalation where the polymer chains diffuse into the space between the clay galleries. This process can be carried out through a conventional melt-compounding process [6, 4].

Exfoliated and homogeneous dispersions of the silicate layers can be obtained in a straightforward manner when the polymer contains functional groups, for example, amide or imide groups [48, 49]. This is due to the fact that the silicate layers of the clay have polar hydroxyl groups, which are compatible with polymers containing polar functional groups [50]. Compatibilizers are usually small molecules (such as oligomers) containing polar groups that facilitate the intercalation of polymers between the silicate layers. As intercalation proceeds, the interlayer spacing of the clay increases, and the interaction of layers weakens. The intercalated clays containing the oligomers contact the polymer under a strong shear field. If the miscibility of the oligomer with the polymer is good enough to disperse at the molecular level, the exfoliation of the intercalated clay should occur. If miscibility is not good, phase separation occurs with no exfoliation.

Rheological studies of PET nanocomposites are not ample, but show very interesting features. In the low frequency range, the nanocomposites display a more elastic behavior than that of PET. It appears that there are some physical network structures formed due to filler interactions, collapsed by shear force, and after all the interactions have collapsed, the melt state becomes isotropic and homogeneous. Linear viscoelastic properties of polycaprolactone and Nylon-6 [51] with MMT display a pseudo-solidlike behavior in the low frequency range of the spectrum, consisting of power-law dependence of the moduli with frequency. If shear flow is applied before, the magnitude of the moduli decreases in the aligned sample, implying that the weak interactions are destroyed by the flow. Nonterminal low frequency rheological behavior has also been observed in ordered block copolymers and smectic liquid crystalline small molecules [52, 53].

In highly interactive polymer–particle systems, solidlike yield behavior can be observed even at temperatures above the glass transition temperature of the polymer [54]. Polymer molecules can adopt stretched configurations that allow them to adsorb to the surfaces of many particles. Relative motion between polymer chains is retarded by immobilization due to polymer confinement between nanoparticle surfaces. The equilibrium thickness of the immobilized polymer layer is of the order of the radius of gyration of the molecule. Filler particles can be regarded as hard cores surrounded by immobilized polymer shells of comparable size.

According to small-angle neutron scattering (SANS) and birefringence experiments by Schmidt et al. [55–57], the influence of shear on viscoelastic-polymer–clay solutions gives rise to an alignment of the platelets along the flow direction and with increasing shear the polymer chains start to stretch. Polymer chains are in dynamic adsorption–desorption equilibrium with the clay particles to form a network. This network is highly elastic, since cessation of shear flow leads to fast recovery.

Another example of network formation is found in PEO (poly(ethylene oxide))–silica systems [58, 59]. At relatively small-particle concentrations, the elastic modulus increases at low frequencies, suggesting that stress relaxation of these hybrids is effectively arrested by the presence of silica nanoparticles. This is indicative of a transition from liquidlike to solidlike behavior. At high frequencies, the effect of particles is weak, indicating that the influence of particles on stress relaxation dynamics is much stronger than their influence on the plateau modulus.

A noteworthy finding has been that all the materials show two distinct relaxation dynamics, a fast and a slow relaxation [60]. The fast mode corresponds to relaxation of bulky polymer molecules, while the slow mode is related to relaxation of the filler structure with much longer time scales. As silica particles are physically connected with adsorbed polymer molecules, the formed polymer–particle network is a temporary physical network. On a long time scale, relaxation of this network occurs when immobilized polymer molecules connecting silica particles become free, via dissociation from silica particles or disentanglement from other immobilized polymer molecules.

Another interesting observation [61] is that remarkable increases in the elastic modulus at low frequency with low values of the molecular weight reflect the fact that an elastic network is formed due to the presence of the clays.

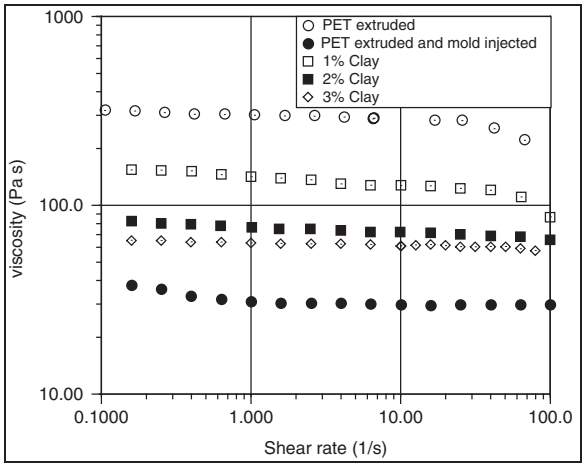

Figure 31.1 The processing of PET leads to loss of viscosity, while the addition of clays increases the viscosity at low contents. Extrusion screw speed is 50 rpm. Mold injection temperature is 7 °C. The tests were made in a rheometer with parallel plates of 25 mm diameter. *Source*: Reproduced with permission from Sánchez-Solís A, Romero I, Estrada MR, Calderas F, Manero O. Polym Eng Sci 2004;44:1094 [61]. Copyright 2004 John Wiley and Sons, Inc.

On the other hand, another remarkable result is that the largest increases in the mechanical properties are observed in samples where the viscoelastic properties are of small magnitudes and have some of the lowest molecular weights. It seems that nanocomposites behave drastically different under tension as opposed to shear. This is advantageous with regard to molding operations, where the viscosity is low and the mold fills conveniently (Figs 31.1 and 31.2).

For example, the observed decrease in the shear viscosity with the addition of MAH and PENTA leads to lower pressure in the filling of the mold in the mold-injection operation. In fact, the injection pressure diminishes from 40,680 kPa for PET to 24,822 kPa in the system PET–clay–MAH (1 wt%) and to 13,790 kPa in the system PET–clay–PENTA under the same processing conditions. This corresponds to a threefold decrease in the viscosity. However, it is necessary to point out that the viscosity curves reported are built from simple shear rheometric flows. In the actual process operation, the fluid that fills the mold is subjected to a nonhomogeneous stress field, which is likely to develop slip at the walls and another complicated flow behavior [62]. In these circumstances, the *in situ* viscosity is probably lower than that measured in the rotational rheometer. Measurements of pressure drop versus flow rate made on the fluid that enters the mold would surely provide a more reliable value of the "process viscosity," and hence a better evaluation of the effect of the nanoparticles on the flow behavior of PET.

31.2.2 PET–PEN/Clay Nanocomposites

PET and PEN form immiscible mixtures. Improved miscibility can be obtained by performing a transesterification reaction between both ingredients to produce copolyesters, which act as compatibilizers in the interface of the blend. This reaction, when carried out in a melt extruder, depends strongly on temperature and residence time, in particular, within 50–80 wt% PEN content [63]. Physical and mechanical properties of the resulting blend depend on the degree of transesterification and also on the resulting copolymer

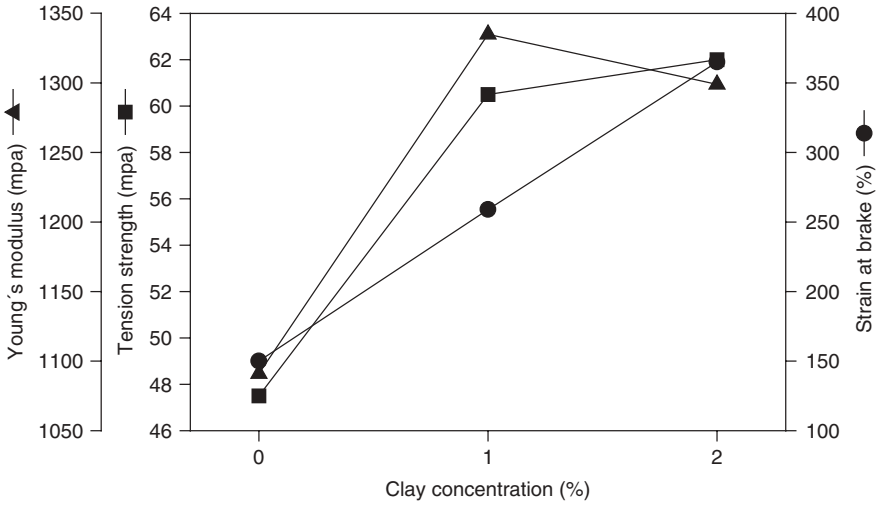

Figure 31.2 Mechanical properties of two modified clays, Clay-MAH and Clay-PENTA, in a 3–1 proportion are shown. Tension strength, Young's modulus, and strain at brake of PET matrix were improved by 18%, 30%, and 140% with 1% clay content, respectively. *Source*: Reproduced with permission from Sánchez-Solís A, Romero I, Estrada MR, Calderas F, Manero O. Polym Eng Sci 2004;44:1094 [61]. Copyright 2004 John Wiley and Sons, Inc.

microstructure, that is, whether it contains block or random substructures.

A great deal of attention on PET/PEN blends has been paid to elucidate the type of kinetics of the transesterification reaction, and, in particular, reversible second-order kinetics has been found in solution [64]. On the other hand, the reaction kinetics is strongly affected by terminal hydroxyl groups when the reaction is carried out in a mixing chamber [65]. In the same device, studies on the thermal, rheological, and mechanical properties for blends with 25, 50, and 75 wt% of PEN content have also been reported [66]. By using a twin-screw extruder, a block copolymer may be obtained via melt extrusion when the PEN content is 20 wt% [67].

From the industrial point of view, PET–PEN blends are attractive in the production of bottles for carbonated liquids filled at high temperatures. PEN imparts the blend a higher resistance to gas diffusion, better mechanical properties, and increased glass transition temperature (T_g). However, these benefits are partly offset by the cost of PEN, and for this reason, PEN contents in the blend higher than 20 wt% are not suitable. Besides, there are some problems in the production of this blend, since transesterification is promoted in systems with similar viscosity [68], but this requirement is difficult to meet since melt viscosity of the ingredients can be widely different. Another problem is that agents that promote miscibility can only be processed at small concentrations, of the order of 2 wt%; otherwise, mechanical properties are negatively affected [69]. Furthermore, for certain concentrations of the ingredients in the blend and the preparation method of the sample, for instance, film under pressure and quenching, some properties increase (such as tensile strength), but others decrease (such as Young's modulus) [70]. On the other hand, when the sample film is bioriented, both tensile strength and modulus improve [71]. It seems that the full relationship between transesterification and mechanical properties is not well understood yet because of the numerous factors and variables that affect this relationship.

Finally, shear viscosity is strongly affected by the clay in the blends, especially at high PEN contents. A lubricating effect rather than a filler effect reveals the possibility that the clay is not well dispersed in the polymer blend, and migration of particles in the flow to the wall region can explain the observed reduction in shear viscosity. When MMT clay is mixed with crystallizable polymers such as polyesters, some processing problems arise because the crystallization process is modified by nucleation effects induced by the nanoparticles. Moreover, these particles also influence the kinetics of transesterification between PET and PEN, besides other factors such as the reaction time and extruder processing temperature. In Reference 72, a quaternary alkyl ammonium compound (C18) and MAH were used to modify the surface properties of the clay particles. Thereafter, the particles were mixed with PET and PEN to produce blends whose properties were examined. The PET–PEN/clay–C18 blend possesses a higher proportion of amorphous phase, because of the restriction to the normal crystallization process due to the particles, as evidenced in the low value of the crystallization enthalpy.

In the transesterification reaction, clay–C18 induces the largest proportion of NET (naphthalate-ethylene-terephthalate) groups as opposed to clay–Na^+, which produces 22 times less NET groups. In spite of the fact that clay–Na^+ is hydrophilic, the surfaces of all samples possess a hydrophobic character. This clay is highly incorporated into the polymer and presumably has a low concentration at the surface, as evidenced in the receding contact angle results that show a predominantly hydrophobic character of the surface. This blend also presents a solidlike behavior, as disclosed by the values of the storage modulus in the low frequency range of the spectrum, which provides evidence for the presence of a high entanglement density and large polymer–particle interactions (Fig. 31.3).

The rheological behavior of these materials is still far from being fully understood but relationships between their rheology and the degree of exfoliation of the nanoparticles have been reported [73]. An increase in the steady shear flow viscosity with the clay content has been reported for most systems [62, 74], while in some cases, viscosity decreases with low clay loading [46, 75]. Another important characteristic of exfoliated nanocomposites is the loss of the complex viscosity Newtonian plateau in oscillatory shear flow [76–80]. Transient experiments have also been used to study the rheological response of polymer nanocomposites. The degree of exfoliation is associated with the amplitude of stress overshoots in start-up experiment [81]. Two main modes of relaxation have been observed in the stress relaxation (step shear) test, namely, a fast mode associated with the polymer matrix and a slow mode associated with the polymer–clay network [60]. The presence of a clay–polymer network has also been evidenced by Cole–Cole plots [82].

The nanocomposite PET–PEN/MMT clay was studied under steady shear, instantaneous stress relaxation, and relaxation after cessation of steady flow [83]. Relaxation times of the slow mode in instantaneous stress relaxation were longer for the systems that have presumably permanent crosslinking networks (PET–PEN) or dynamic networks (PET–PEN–MMT). These results are consistent with those found in relaxation after cessation of flow (Fig. 31.4). Nanoclay addition somehow restricts the slow relaxation (due to polymer–particle interactions). The nanocomposite exhibits lower steady-state viscosity as compared to the polymer–matrix system. This is thought to be caused by polymer–polymer slipping, as revealed by the SEM observations (Fig. 31.5a and b).

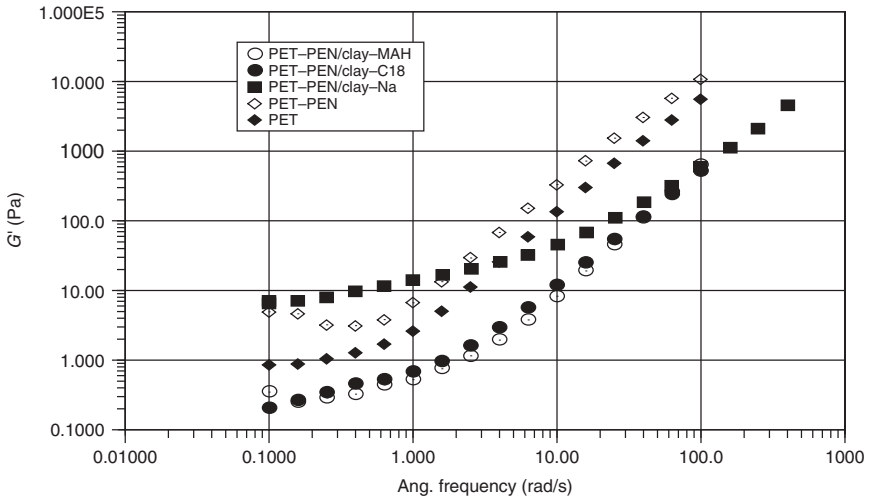

Figure 31.3 Variation of the storage modulus with frequency for PET/PEN–clay systems. *Source*: Reproduced with permission from Sánchez-Solís A, García-Rejón A, Estrada M, Martínez-Richa A, Sánchez G, Manero O. Polym Int 2005;54:1669 [72]. Copyright 2005 John Wiley and Sons, Inc.

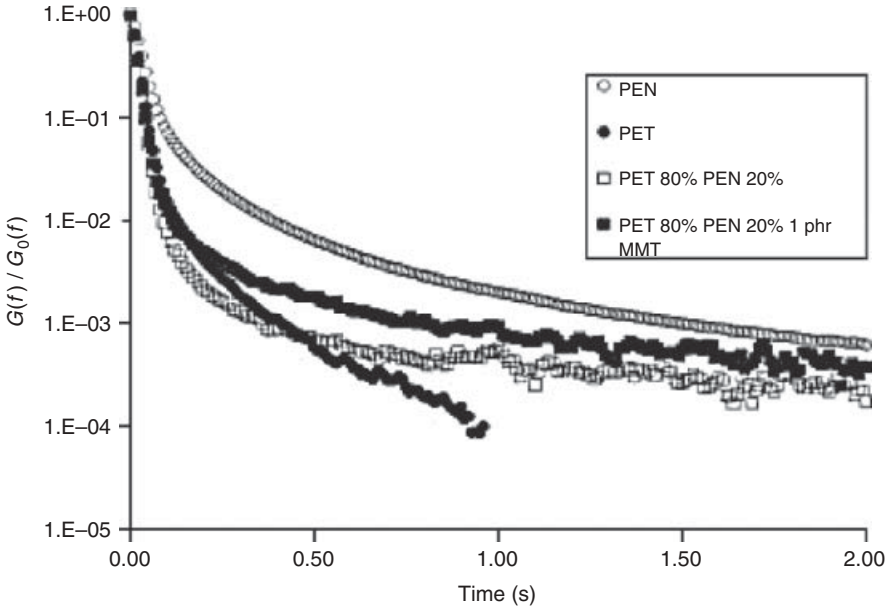

Figure 31.4 Stress relaxation curves after cessation of steady shear flow for the PET/PEN–clay systems (shear rate is 10 s^{-1}). *Source*: Reproduced with permission from Calderas F, Sánchez-Solís A, Maciel A, Manero O. Macromol Symp 2009;283:354 [83]. Copyright 2009 Wiley-VCH Verlag GmbH & Co. KGaA.

31.2.3 Polyester Resin/Clay Nanocomposites

Unsaturated polyester resins are produced by a crosslinking reaction in solution of a prepolymer dissolved in styrene initiated with peroxides. This curing reaction renders an insoluble and infusible crosslinked matrix with high rigidity, but fragile. This matrix is usually reinforced with glass fibers or fillers of micrometric size. Since the mechanical properties of such materials depend strongly on the interaction among phases, attention has been given to the analysis of matrix–filler interactions.

The effect of high shear mechanical mixing and sonication methods on the physical properties of the nanocomposites has been analyzed [84] using modified clays with a quaternary ammonium salt and calcium carbonate [85] and silane-treated clays [31]. Although the nanoclay is usually chemically modified to make it organophilic and compatible with the polymer matrix, untreated MMT was

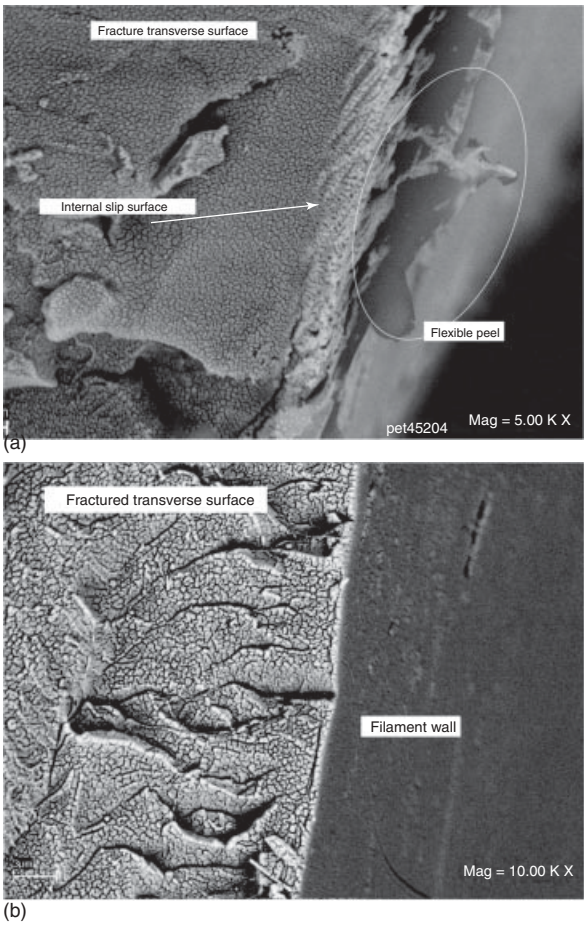

Figure 31.5 SEM micrograph of the edge region of a capillary filament: (a) blend with clay and (b) blend without clay. *Source*: Reproduced with permission from Calderas F, Sánchez-Solís A, Maciel A, Manero O. Macromol Symp 2009;283:354 [83]. Copyright 2009 Wiley-VCH Verlag GmbH & Co. KGaA.

also used, taking advantage of its high swelling capacity in polar liquids such as water or alcohol, allowing the expansion of the interlaminar spacing and the subsequent intercalation or exfoliation of the clay after polymerization.

Exfoliation of MMT in the polymer matrix has been shown to occur through a process called *slurry compounding*, in which the MMT swells in water and then is mixed with Nylon-6 under extrusion [86]. Other techniques include the addition of MMT to water and the subsequent replacement of water by alcohol or acetone with further addition of a silane agent to modify the clay and make it compatible with the polymer matrix [87–89]. Intercalated nanocomposites were also obtained by slurry compounding introducing an epoxy monomer in the hydrated MMT galleries [90].

Preparation of nanocomposites using the slurry compounding process has been carried out with Nylon and epoxy resins. In Reference 91, this method is implemented to obtain polyester resin–clay nanocomposites. The influence of MMT slurry on the crosslinking reaction with the unsaturated polyester resin, and the effect of the clay hydration on the thermal and mechanical properties of the resulting nanocomposites have been analyzed. In addition, changes with respect to the pristine polyester resin on the gelation temperature and morphology of the nanocomposites prepared with this novel method were also analyzed in detail.

The procedure to obtain nanocomposites based on unsaturated polyester resins leads to improvements in the order of 120% in the flexural modulus, 14% in flexural strength and 57% increase in tensile modulus with 4.7% of clay slurry content. Thermal stability augments and the gelation temperature increases to 45 °C, as compared to that of the resin (Fig. 31.6). It seems that adding water to the MMT allows better intercalation of polymer chains into the interlamellar space. Because clay is first suspended in water, this improves dispersion and distribution of the particles in the resin matrix. Longer gelation times lead to more uniform and mechanically stronger structures and to yield stresses (Fig. 31.7). Enhanced polymer–clay interactions are revealed by XPS in this case (Fig. 31.8).

31.3 POLYOLEFIN/CLAY NANOCOMPOSITES

31.3.1 Polyethylene/Clay Nanocomposites

As pointed out before, the polymer may be functionalized with polar groups to enhance compatibility with the modified clay. Bellucci et al. [92] have reported that the formation of polymer–clay nanocomposites depends mostly on the polymer properties, clay characteristics, and type of organic modifier.

In the case of LDPE–clay nanocomposites, the mechanical behavior does not depend only on the degree of exfoliation or the clay content but also on the presence of substantial amounts of compatibilizer [93, 94]. Besides the chemical modification of the clay, it is then necessary to turn the polymer matrix more polar with the grafting of polar groups. Traditionally, MAH has been used as the polar group to induce compatibility due to the high reactivity of the anhydride group.

The use of organically modified clays and PE grafted with MAH allows for the production of polymer nanocomposites with improved mechanical properties [95, 96]. Liang et al. [97] reported improvements in the mechanical properties when the HDPE concentration is larger than 6 wt%. Wang et al. [98] reported that the most important factors for improved PE–clay nanocomposites are the chain length of the intercalant (chains with more than 16 carbon atoms) and low amount of grafting (0.1 wt%). Chrissopoulos et al. [99] observed that exfoliated structures are obtained when the proportion of MAH-*g*-PE/clay is

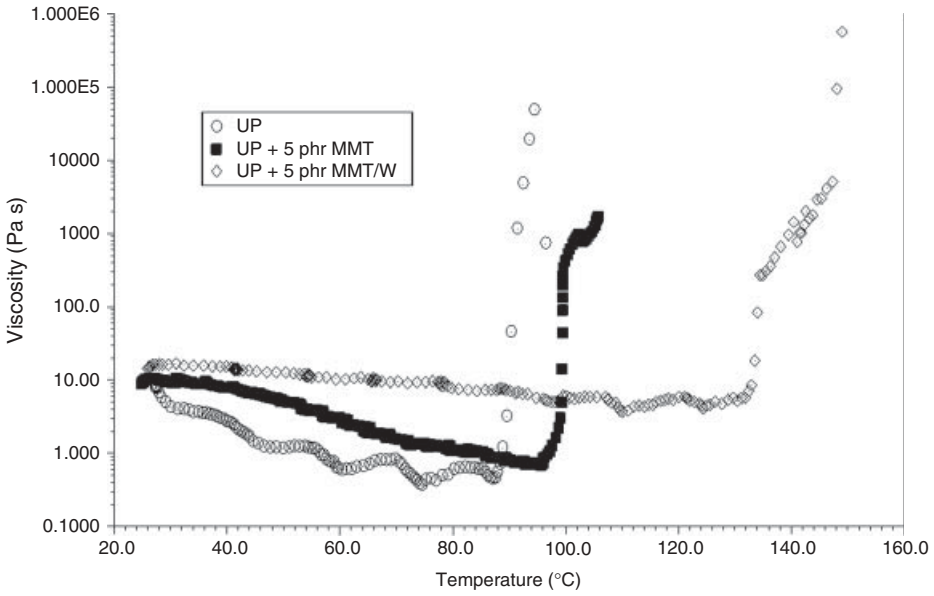

Figure 31.6 Shear viscosity versus temperature for an unsaturated polyester resin (UP)–clay slurry indicating the temperature for the onset of the gelation reaction. *Source*: Reproduced with permission from Rivera-Gonzaga JA, Sanchez-Solis A, Manero O. J Polym Eng 2012:32,1 [91]. Copyright 2012 De Gruyter.

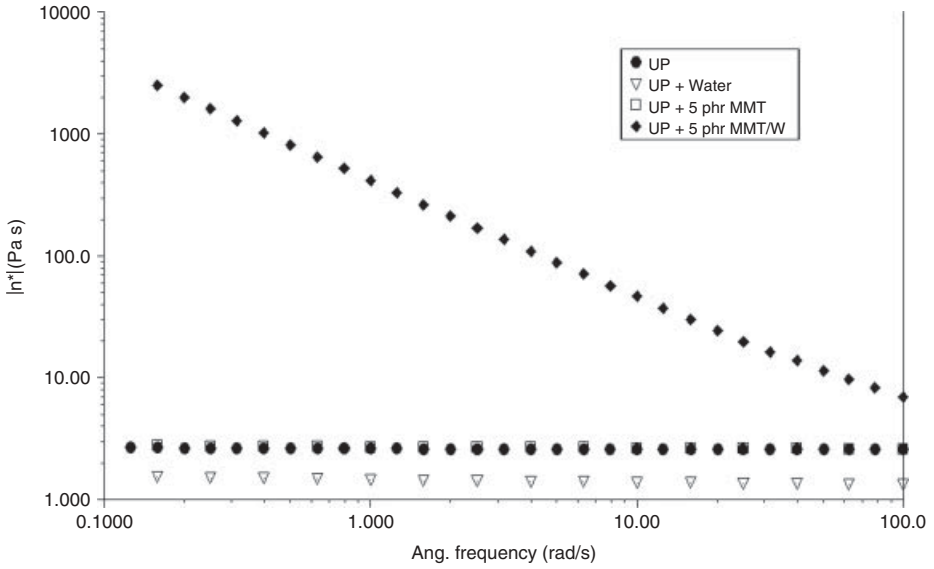

Figure 31.7 Complex viscosity as a function of oscillation frequency for an unsaturated polyester resin–clay slurry system. *Source*: Reproduced with permission from Rivera-Gonzaga JA, Sanchez-Solis A, Manero O. J Polym Eng 2012:32,1 [91]. Copyright 2012 De Gruyter.

larger than 4.5/1. Arrunvisut et al. [100] further agreed in that hydrogen bridging between the MAH-grafted groups and hydroxyl groups from the clay edges favor phase compatibility.

Nanocomposites exhibiting improved mechanical properties reveal strong polymer–clay interfacial adhesion, increasing with the exfoliation degree of the clay [96, 101]. However, in addition to this, there is evidence of improvements found with partial exfoliation [102, 103] of tactoids formed by 10–20 lamellas, due to required flexibility of the dispersed particles. Interfacial interactions are of fundamental importance in the structure and properties of nanocomposites. Lee et al. [104] proposed that the interactions of the polar maleic groups grafted to PP with hydroxyl groups of

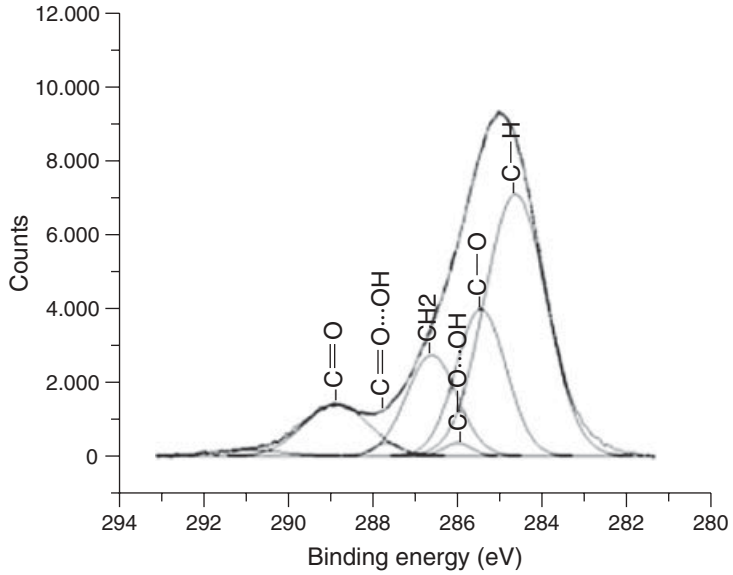

Figure 31.8 XPS of the UP-MMT/W system revealing interactions between C═O···HO and C–O···HO groups. *Source*: Reproduced with permission from Rivera-Gonzaga JA, Sanchez-Solis A, Manero O. J Polym Eng 2012:32,1 [91]. Copyright 2012 De Gruyter.

the clay are of the van der Waals type and no chemical reactions are likely. Xie et al. [105] suggested, alternatively, a possible formation of links between the maleic groups of PP and the ammonium groups in the clay galleries. In addition, Walter et al. [106] mentioned the possibility of a reaction between the MAH and octadecyl amine, used to modify the clay.

The ternary blends mentioned, nonetheless, are used in stretch and thermoshrinkable films in the packing industry and in the agricultural uses to protect crops. In this regard, an improved understanding of the particle–polymer interactions may motivate the formulation of new materials with specific properties.

In Reference 107, the effect of grafting of a polar group (MAH) onto LDPE chains and the chemical modification of clay particles with 2,6-diaminocaproic acid (L-lysine monohydrochloride) to produce nanocomposites with a matrix composed of a ternary blend of PEs (LDPE, LLDPE, and HDPE) was studied in detail. X-ray diffraction was used to determine the exfoliation degree of the clay. Morphological features were revealed by scanning electron microscopy and thermal analysis disclosed the thermal stability of the samples. Comparative analyses of the mechanical (under tension) and rheological properties of the nanocomposites were carried out as well.

It was shown that the PE ternary blend composed of 25%, 42%, and 33% HDPE, LLDPE, and LDPE, respectively, possessed the required mechanical properties to resist tear forces in films for packing and agricultural uses. MAH grafting on LDPE (0.36%) in addition to L-lysine-modified clay induced a large clay-grafted polymer interaction. With respect to the reference ternary blend, the resulting system presented increases of 13% in tensile strength, 140% strain at break, 111% strength at break, and 11% tear strength with no substantial changes in the modulus. Rheological data revealed a shear-thinning behavior in viscosity consistent with high orientation at high shear rates, assisted by the clay particles. The decrease in the slope of the storage modulus in the low frequency range under oscillatory shear manifested high clay particle-grafted LDPE interaction. The entanglement density and the relaxation time were strongly affected by the presence of the modified clay particles if no MAH-grafted chains were present to promote polymer–clay-enhanced interactions.

The improvement in the mechanical properties of the nanocomposite LDPE-*g*-MAH/bentonite -L-lysine as compared to those of the blend HDPE–LLDPE–LDPE were explained in terms of a good exfoliation degree and uniform dispersion of the platelets in the polymer matrix. To prove this relationship, diffraction X-ray spectra, TEM, and rheological tests revealed changes in the morphology and linear viscoelastic properties identified with the compatibilizer action through the polar groups. The nanocomposite synthesis was possible even at very low grafting (0.45 wt%) and with small amounts of organo-clay (0.49%).

31.3.2 Polypropylene/Clay Nanocomposites

PP is a commodity polymer used in mostly automobile applications (bumpers and interiors) and in packaging and food containers. Mica and talc are used as fillers (from 20% to 40%) to improve dimensional stability and mechanical

properties. Clays of several kinds can enhance stiffness and resistance at much lower loadings. They can also yield improved barrier resistance and flame retardance. In the case of PP, from 5 to 10 wt% clay content, improvements in the polymer properties are found. Melt compounding has been used by Okada et al. [6, 7, 108] for PP -layered silicate nanocomposites.

The interactions between the oxygen atoms of the clay surface and the polymeric compatibilizer must be stronger than the interactions between the clay surface and the surfactant to obtain delamination of the silicates [109]. The length of the surfactant chain is an important variable that influences the level of exfoliation. In the case of alkyl amides, the chain must contain more than eight carbon atoms for the clay to be exfoliated in PP. Some authors [110] have found that with 1 wt% MA content in PP-*g*-MAH, a 2 : 1 ratio is adequate to obtain exfoliation of the clay. A major limitation to the grafting reaction is polymer degradation. As the grafting content increases, the molecular weight of PP is reduced and, hence, the mechanical properties.

Procedures for melt compounding usually mix the clay with the functionalized grafted polymer (PP-*g*-MAH) in a 1 : 3 proportion and this concentrate may be thereafter mixed with PP to get a final 80/15/5 PP/PP-*g*-MAH/clay proportion. Other procedures suggest first mixing the grafted polymer with the clay for exfoliation and thereafter these ingredients are mixed with PP with peroxides. A third method suggests the incorporation of clay to a mixture of PP, PP-*g*-MAH, and surfactant using a ratio of 6 : 1 of PP-*g*-MAH to clay [111]. An example of the improved adhesion of fibers to the PP matrix due to the compatibilization action by the polar groups is shown in Figures 31.9 and 31.10.

The rheological properties of the nanocomposites show an increase of the elastic modulus with MAH content of the grafted polymer and also an increase of the modulus with clay content. Under small amplitude oscillatory flow, plots of the dynamic viscosity with complex modulus show that in composites, the dynamic viscosity increases sharply with decreasing stress, in fact revealing the presence of a yield stress in clay systems as compared to silicate-free melts [112]. Under extensional flow, the nanocomposites display strain hardening, which is absent in the PP matrix or in the grafted PP. Orientation of the platelets normal to the flow in uniaxial extension contrasts to that under biaxial extension, where the platelets are now positioned along the flow direction [113]. When the nanocomposites were extruded through a converging die section, with strong uniaxial extensional flow, the platelets are in this case oriented along the flow direction. Research on mechanical properties and fire-retardant properties may be found elsewhere [114, 115].

31.4 POLYSTYRENE/CLAY NANOCOMPOSITES

31.4.1 HIPS/Clay Nanocomposites

Improvements in the reduction of flammability of polymers with low clay contents and better processability have been reported, in addition to reductions in the concentration of toxic vapors produced in the combustion stage [116–120]. In connection to their flame-retardant properties, exfoliated nanocomposites based on PP [121, 122, 115, 123], PS [115, 123, 124], poly(ethylene–vinyl acetate) [125, 126], styrene–butadiene rubber [127], PMMA [128], polyesters [129], acrylonitrile butadiene styrene [130], and polymeric foams [131] have been the subject of increasing attention.

The flame-retardant mechanism involves the formation of a carbonaceous char layer on the surface of the burning material due to the presence of clay particles that act as an insulating barrier. The extent of this layer depends, among various factors, on the concentration, distribution, dispersion, and compatibility of the particles with the polymer. Phosphorous compounds are among the most popular nonhalogenated flame-retardant agents used with thermoplastic polymers, thermosets, textiles, and coatings. In these systems, the mechanism of flame-retarding depends mainly on the type of phosphorous compound and on the polymer microstructure [132].

In some cases, such as in the PET system, it is possible to exfoliate the clay by extrusion without previous clay treatment [61]. In Reference 133, a comparative study is carried out on the use of pristine-layered MMT-Na^+ and MMT-Na^+ intercalated with triphenyl phosphate (TPP), as flame-retardant agents when mixed with HIPS. Results of the burning rate, mechanical, impact, and rheological properties of the HIPS nanocomposite were presented. The HIPS-MMT clay (MMT-Na^+) blends present increasing burning rate with clay content as compared to that of HIPS alone, even at high clay concentrations. TPP acts as a flame-retardant agent when it is intercalated in the clay galleries. These results have been explained on the basis of the combined effect of decreasing viscosity of the flowing blend and temperature.

In the blends with TPP (4.7%), the mechanical properties of HIPS are retained. For TPP concentrations larger than 5.6%, the material self-extinguishes as dripping of the burning material occurs. In the MMT-*i*-TPP blends, the degradation temperature of the nanocomposite compared with that of HIPS is not affected. MMT-*i*-TPP blends work as a fire-retardant agent, although in the extrusion process the clay with TPP is not exfoliated.

31.4.2 HIPS-PET/Clay Nanocomposites

HIPS is widely used in the audio, video, automotive, aircraft industries, and in electric appliances, among others.

Figure 31.9 Mix of PP-PP-*g*-MAH with glass fibers. Adhesion between the fibers and matrix is poor.

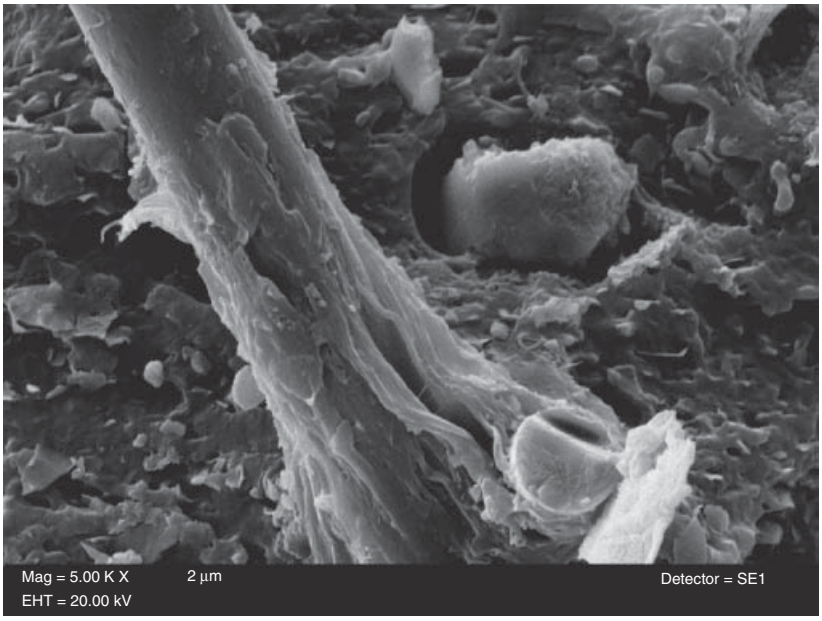

Figure 31.10 Mix of PP/PP-*g*-MAH/clay-L-lysine. Adhesion of the fibers to the matrix is apparent, brought about by the change in surface tension with the modified clay.

Small rubber particles embedded in the PS matrix provide high impact resistance [134, 135]. However, this polymer is highly flammable as it is exposed to fire, due to its chemical structure, where aliphatic groups bound to aromatic moieties provide hydrogen to the combustion reaction without forming any char layer that may prevent fire propagation [132, 136].

To improve flame retardation in HIPS, agents formulated from halogenated compounds have been traditionally used [137, 138]. These compounds form, nevertheless, highly toxic vapors during the combustion process. Recently, alternative flame-retardant compounds have been developed, ensuring that no toxic vapors are expelled, presenting an augmented thermal stability. Furthermore,

reports have highlighted that a carbonaceous layer is easily formed during combustion, acting as a barrier to energy transfer and mass loss [118–120]. Attention in the recent literature has been given to the flame retardation properties of polymer nanocomposites [139–141].

In Reference 142, PET was used in blends with HIPS and modified MMT clay. The use of PET was justified since this polymer self-extinguishes under fire. In addition to study the flame-retardant properties of the HIPS–clay and HIPS–PET–clay systems, mechanical and rheological properties were measured to provide explanations on the mechanism by which the polymer nanocomposites inhibit flame propagation. The mechanism proposed considered that clay particles stay at the interface between both polymers, since the interfacial tension of the particles with HIPS is larger than that with PET. The clay particles in the PET microspheres then promote the formation of the carbonaceous layer that leads to diminishing burning rate (Figs 31.11 and 31.12).

In Reference 143, the analysis of the processes aimed at reducing the flammability properties of HIPS with the use of clays and a nonhalogenated flame-retardant

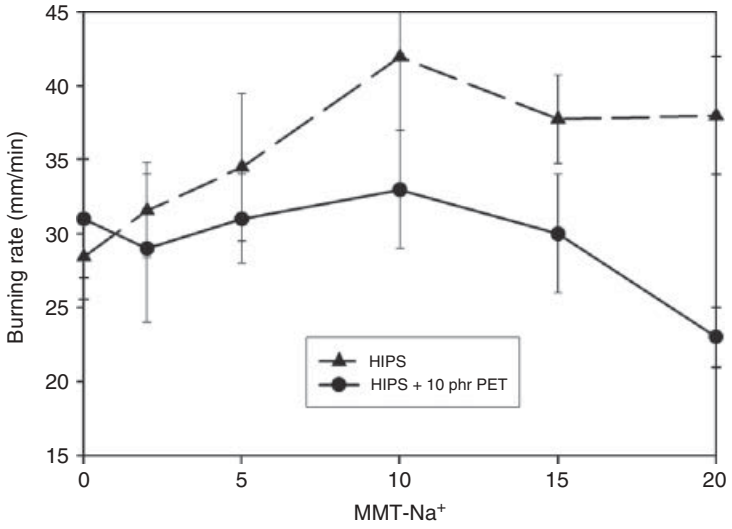

Figure 31.11 HIPS–clay and HIPS–PET–clay systems. Burning rate as a function of clay content. *Source*: Reproduced with permission from Rivera-Gonzaga JA, Sanchez-Solis A, Manero O. J Polym Eng 2012:32,1 [91]. Copyright 2012 De Gruyter.

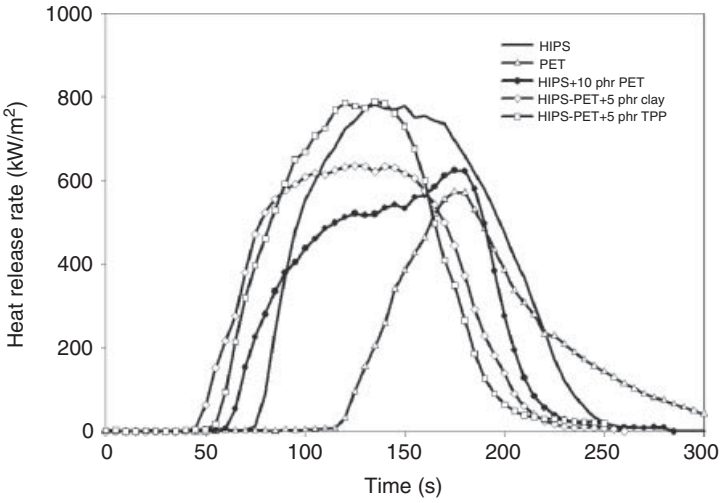

Figure 31.12 Heat release rate plotted with time for HIPS, PET, HIPS–PET (10 phr), HIPS–PET(10 phr) + 5 phr clay; and HIPS–PET(10 phr) + 5 phr TPP. *Source*: Reproduced with permission from Sanchez-Olivares G, Sanchez-Solis A, Manero O. Int J Polym Mater 2008;57:417 [142]. Copyright 2008 Taylor & Francis.

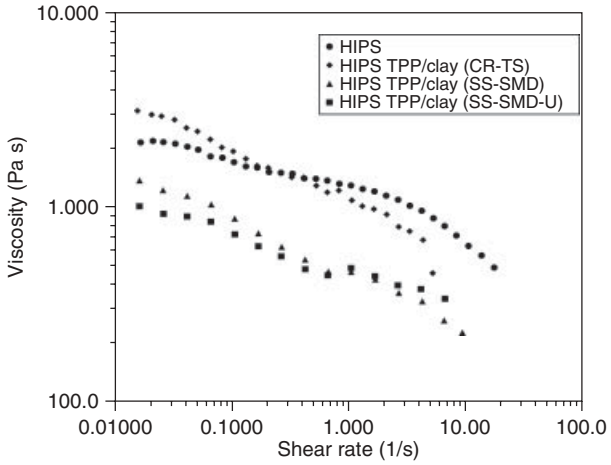

Figure 31.13 Shear viscosity as a function of the shear rate for the HIPS–TPP/clay blends. CR-TS, twin-screw counter-rotating extruder; SS-SMD, single-screw extruder with the static mixing die; SS-SMD-U, single-screw extruder with the static mixing die and sonication. *Source*: Reproduced with permission from Sanchez-Olivares G, Sanchez-Solis A, Camino G, Manero O. Express Polym Lett 2008;2:569 [143]. Copyright 2008 BME-PT.

additive, maintaining the original mechanical properties of HIPS, mainly the impact resistance, was carried out. The use of different extrusion processes was intended to improve clay and flame-retardant agent dispersion to reduce HIPS flammability. The extrusion processes considered include intermeshing counter-rotating twin-screw, single-screw with a static-mixing die, and the latter with sonication transducers placed on the die itself (Fig. 31.13).

This study demonstrated that the HIPS–TPP/clay blend properties (flammability, combustion, thermal, rheological, and mechanical) depend on the dispersion and distribution of the particles into the polymer matrix. Three extrusion processes were considered to produce different degrees of particle dispersion. When this was good (single-screw with the static mixing die process), the peak in the heat release rate diminished in cone-calorimetric tests. The contrary occurred (twin-screw process) when particle dispersion was not uniform (Figs 31.13 and 31.14).

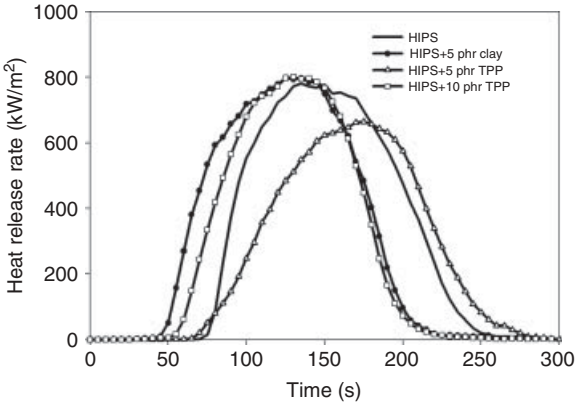

Figure 31.14 Heat release rate plotted with time for HIPS and blends with clay and TPP. *Source*: Reproduced with permission from Sanchez-Olivares G, Sanchez-Solis A, Camino G, Manero O. Express Polym Lett 2008;2:569 [143]. Copyright 2008 BME-PT.

31.5 POLYMER/CARBON BLACK NANOCOMPOSITES

31.5.1 PET– PMMA/Carbon Black Nanocomposites

The electrical properties of insulating polymers may be modified when they are mixed with conductive particles such as metal powder, CB, graphite, or an intrinsically conducting polymer. Among the available fillers, the most popular is carbon CB. The selective localization of CB particles in multiphase polymeric materials is a favorable condition for obtaining heterogeneous microdispersion of CB [144–152]. It was found that CB distributes unevenly in each component of the immiscible polymer blend. Two types of distribution were observed: in the first, CB was distributed predominantly in one phase of the blend homogeneously. In the second, the conductive particles concentrated at the interface of the two phases. The conductivity of these composites was determined by two factors: the preferential concentration of CB in one phase and the structural continuity of this phase. This double percolation, that is, percolation of the polymer phases and percolation of the CB particles, or cocontinuous phase morphology, depicts especially low resistivity values. Interfacial free energies, mixing kinetics and viscosities, and polymer polarity and crystallinity are important factors governing the selective localization of CB. The production of low conductive materials with permanent antistatic properties using polymeric alloys has been given attention by Lee [153].

In Reference 154, PMMA was selected as it is immiscible with PET. The description of the electroconductive properties of this immiscible polymer blend filled with CB was carried out. To properly analyze the results obtained, models that predicted the selective location of CB in the blend were considered. The presence of CB extensively modified the rheological and conductive properties of the blend. Resistivity decreased similarly in both PET and PMMA with CB concentration. However, the immiscible polymer blend extensively modified this behavior because resistivity became a function of morphology and location of CB in the polymers. Viscosity was observed to be a strong function of PET content at high CB concentrations. Indeed, resistivity decreases continuously (a drop of seven decades) for 20% CB (PET basis) from 0% to 60% PET content. The same behavior (similar slope) was observed for 5% CB, but the conductivity curve was shifted to higher PET contents. It was shown that the preferential CB location in

the PET phase is explained on the basis of surface tension values. The polar groups of PET interacted more strongly with the conductive CB particles, resulting in a relatively higher concentration of CB in PET.

31.5.2 PET–HDPE/Carbon Black Nanocomposites

In these systems, it is possible to obtain low percolation thresholds if a double percolation is present, that is, particle and phase percolation. This effect may be observed when the conductive particles, localized preferentially in one polymer phase, have a concentration equal or larger than the electric percolation threshold, and when the host polymer phase is the matrix or continuous phase of the polymer blend [155]. There are several models that describe the electroconductivity of these systems: the effective medium theory, the onset for percolation theory, and thermodynamic models. Sumita's model considers the formation of chainlike conductive structures [151, 156].

The study of electroconductive polymer systems, based on conductive particles and polymer blends, has been quite intensive during the recent past. Gubbels et al. [149] studied the selective localization of CB particles in multiphase polymeric materials (PS and PE). According to these results, the percolation threshold may be reduced by the selective localization of CB. The minimum resistivity was obtained when double percolation (phase and particle percolation) exists in the PS–PE blend. In addition, it was found that the percolation threshold may be obtained at very low particle concentrations, provided that CB is selectively localized at the interface of the blend components. Soares et al. [150] found that the type of CB (i.e., different surface areas) does not affect the conductivity of the blend with 45/55 PS/PIP (polyisoprene) composition.

Blends of PET/HDPE have been treated previously in the literature [157, 158]. These are immiscible, but the addition of compatibilizers improves the mechanical properties of the blend, such as styrene-ethylene/butylene-styrene (SEBS) and ethylene propylene diene monomer (EPDM) [157], MAH [158], Poly(ethylene-stat-glycidyl methacrylate)-graft-poly(acrilonitrile-stat-styrene) (EGMA), poly (ethylene acrylic acid), and maleated copolymers of SEBS, HDPE, ethylene-propylene copolymer (EP). The addition of compatibilizers modifies the rheological properties of blends of PET with HDPE, in such a way that increases in viscosity are observed as the component interactions augment. Changes in crystallization of PET were evaluated in blends with Polyphenylene sulfide (PPS), PMMA, HDPE aromatic polyamides, and copolyesters [159].

CB easily mixes with elastomers and thermoplastics. It is made of colloidal-size particles that provide a good dispersion in the matrix and also good mechanical properties [160, 161]. The manufacturing process of CB involves the thermal decomposition of petroleum or natural gas [162]. The product leaves the oven at high temperature in the form of particle agglomerates with high surface area and with a quasigraphite conformation. The most important properties of CB are structure and surface area. The structure of CB is characterized by the arrangement, distribution and ordering of the particles, which is itself a function of the surface area, and number of particles in each aggregate. The structure is characterized by the value of the absorption of dibutylphthalate (DBP) or by the Brunauer–Emmet–Teller method. In Reference 163, attention was given to the rheological and electroconductive properties of PET/HDPE blends filled with CB. Particular emphasis was given to the effect of different types of CB, comprising different surface areas, structure, and porosity, upon the resulting rheological and electroconductive properties of the blend.

The rheological properties of the blends affect the structural arrangement of particles in the matrix formed by the blend of two immiscible polymers. Particle structure, chemical properties of the surface, morphology of the surface, size, content, and orientation are important factors, besides the properties of the matrix, to obtain conducting blends. Higher viscosities are recorded in the systems with more structured CB samples. CB is preferentially located in the more viscous phase (HDPE) due to the lower interfacial tension between CB and HDPE. In more structured CBs, the percolation threshold is observed to occur at low concentrations of CB particles, in the region of high HDPE content. The system exhibits high conductivity when HDPE is the dispersed phase. In this case it is likely that CB forms conductive pathways either in the dispersed HDPE phase or at the interface between the two polymers.

31.6 NANOPARTICLES OF BARIUM SULFATE

Barium sulfate ($BaSO_4$) has an industrial relevance due to its whiteness, inertness, high specific gravity, and optical properties, such as opacity to UV rays and X-rays [164–167]. It is mainly used as a radio-contrast agent, filler in plastics, extender in paints, coatings and additive in pharmaceutical products, and in printing ink. Nowadays, interest on this material has been renewed with the development of methods to produce nanosized particles, supraparticles of a well-controlled number of nanoparticles and mesocrystals that mimic biomineralization processes.

Among the methods for nanoparticle synthesis, controlled precipitation has the advantage of good reproducibility, low cost, and the use of mild reaction conditions within a relatively simple process. This method can improve the quality of the product in terms of controlling the particle size and the particle size distribution. Concentration, pH, temperature, reaction media, and the introduction of stabilizing agents (chelating agents, polymeric inhibitors, surfactants, and other organic additives) are the most important parameters to promote nucleation and controlled growth.

The control of shapes of $BaSO_4$ has been the object of numerous studies. Li et al. prepared ellipsoidal nanocrystals by using ethylene diamine tetraacetic acid (EDTA) [168], while Yu et al. obtained fibers in presence of sodium polyacrylate [169]. Likewise, using the same agent, Wang et al. have reported a well-established method to obtain cones, fiber bundles as well as elucidating their crystallization and its associated kinetic mechanisms [170, 171]. The kinetics of the crystallization process involves the nucleation and growth rates of the crystal, which are directly dependent on the saturation ratio. This ratio is the driving force for nucleation and growth and determines the induction period along which a stationary cluster distribution is reached and critical nuclei are formed [172]. Judat and Kind proposed a mechanism for $BaSO_4$ formation that involves molecular and aggregative growth [173]. Qi et al. synthesized a variety of well-defined morphologies using double-hydrophilic block copolymers as crystal growth modifiers to direct the controlled precipitation as a function of pH [174, 175]. A possible mechanism for the development of (defect-free growth) bundles of $BaSO_4$ nanofilaments from the amorphous precursor particles by attractive van der Waals forces and crystal multipole forces was proposed (vectorially directing).

In Reference 176, the morphology of $BaSO_4$ nanostructures, synthesized by controlled precipitation, was studied in detail. The influence of the capping agent, pH, reaction media, and aging, on the agglomerate shape, primary, and secondary particle size, was further analyzed. The synthesis of nanometric $BaSO_4$ in dimethyl sulfoxide (DMSO) allows the production of long fibers (Fig. 31.15). HRTEM observations allowed a direct assessment of self-assembled primary barium sulfate nanoparticles, which suggest a brick-by-brick assembling mechanism via hierarchical organization during aging processes. Direct observation of self-assembled primary particles by HRTEM revels that fibers are formed via hierarchical organization of barium sulfate nanoparticles during aging processes (Fig. 31.16).

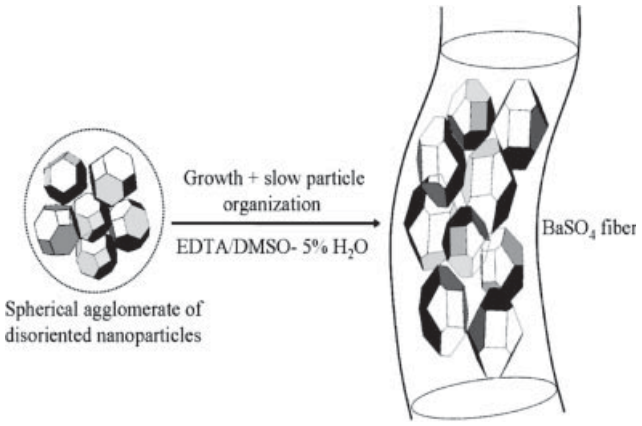

Figure 31.16 Schematic representation of the $BaSO_4$ fiber formation mechanism by electrostatic multipolar interactions. *Source*: Reproduced with permission from Romero-Ibarra IC, Rodriguez Gattorno G, Garcia Sanchez MF, Sánchez Solís A, Manero O. Langmuir 2010;26:6954 [176]. Copyright 2010 American Chemical Society.

31.7 POLYMER/GRAPHENE NANOCOMPOSITES

Graphene–polymer nanocomposites share with other nanocomposites the characteristic of remarkable improvements in properties and percolation thresholds at very low filler contents. Although the majority of research has focused on polymer nanocomposites based on layered materials of natural origin, such as an MMT type of layered silicate compounds or synthetic clay (layered double hydroxide), the electrical and thermal conductivity of clay minerals are quite poor [177]. To overcome these shortcomings, carbon-based nanofillers, such as CB, carbon nanotubes, carbon nanofibers, and graphite have been introduced to the preparation of polymer nanocomposites. Among these, carbon nanotubes have proven to be very effective as conductive fillers. An important drawback of them as nanofillers is their high production costs, which

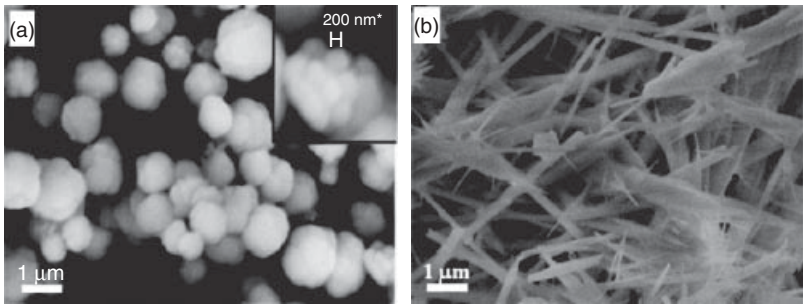

Figure 31.15 BaSO4 aggregates at room temperature: (a) after the reaction and (b) past eight days of aging. *Source*: Reproduced with permission from Romero-Ibarra IC, Rodriguez Gattorno G, Garcia Sanchez MF, Sánchez Solís A, Manero O. Langmuir 2010;26: 6954 [176]. Copyright 2010 American Chemical Society.

impede their mass production of composite materials. In this regard, graphene can provide new means in the field of nancomposite production.

Graphene is considered bidimensional carbon nanofiller with a one-atom-thick planar sheet of sp^2-bonded carbon atoms that are densely packed in a honeycomb crystal lattice. It is regarded as one of the thinnest materials with tremendous application potential. Graphene and polymer/graphene nanocomposites have remarkable properties, among these:

1. *Mechanical Properties*. The tensile strength of graphene is similar or slightly higher than carbon nanotubes, but much higher than steel, Kevlar, HDPE, and natural rubber [178]. Graphene-based polymer nanocomposites exhibit superior mechanical properties compared to the neat polymer or conventional graphite based composites. This is attributed to the very high aspect ratio of the graphene filler.
2. *Thermal Stability and Conductivity*. Thermal degradation temperature of PMMA, PS, and PVA (poly(vinyl alcohol)) nanocomposites shifts up by 10–100 °C. During combustion [179], nanoparticles form a network of char layers that retards the transport of decomposition products. The thermal conductivity of epoxy composites is four times higher than that of the neat epoxy resin with 5 wt% loads.
3. *Dimensional Stability*. Since graphite has a negative thermal expansion coefficient [180], graphene can prevent dimensional changes in polymers when incorporated and oriented appropriately.
4. *Gas Permeation*. Nanocomposites with homogeneously dispersed graphene in the polymer matrix also exhibited good barrier properties [181]. N_2 and He permeation rates were suppressed several-fold by the addition of functionalized graphene.
5. *Electrical Conductivity*. Graphene-based polymer nanocomposites exhibit a several-fold increase in electrical conductivity [182]. These improvements are due to the formation of a conducting network by graphene sheets in the polymer matrix. The maximum or very high electrical conductivity was obtained using a very low graphene loading in different polymer matrices compared to other carbon fillers. Conducting polymer/graphene composites can also be used as electrode materials in a range of electrochromic devices. The polymer/graphene flexible electrode has some commercial applications in LEDs, transparent conducting coatings for solar cells and displays.

31.7.1 Synthesis and Structural Features of Graphene

Graphene can be prepared using four different methods [183]. The first is chemical vapor deposition (CVD) and epitaxial growth, such as the decomposition of ethylene on nickel surfaces. The second is the micromechanical exfoliation of graphite. The third method is epitaxial growth on electrically insulating surfaces, such as SiC, and the fourth is the solution-based reduction of graphene oxide (Fig. 31.17).

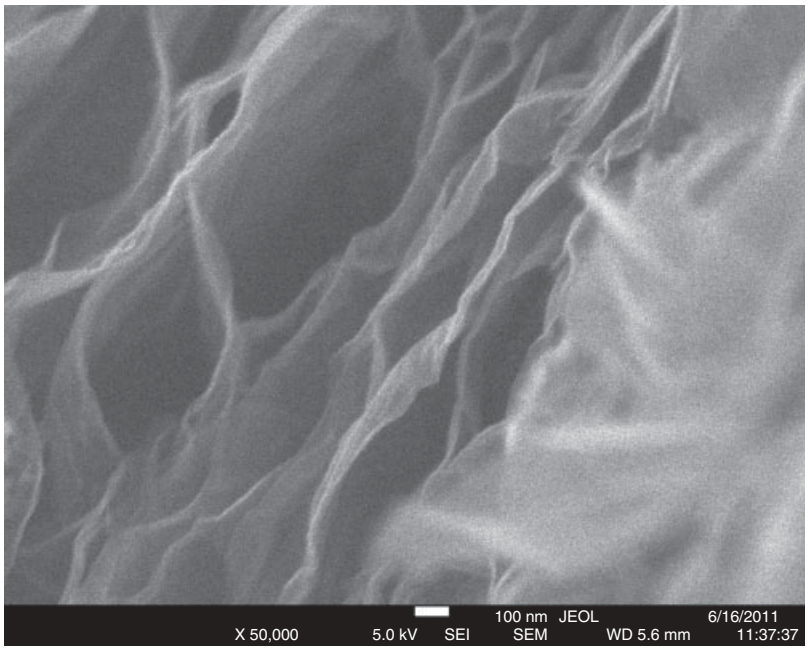

Figure 31.17 HRSEM micrograph of graphene laminates obtained from graphite oxide through the Hummers and Offeman procedure [184].

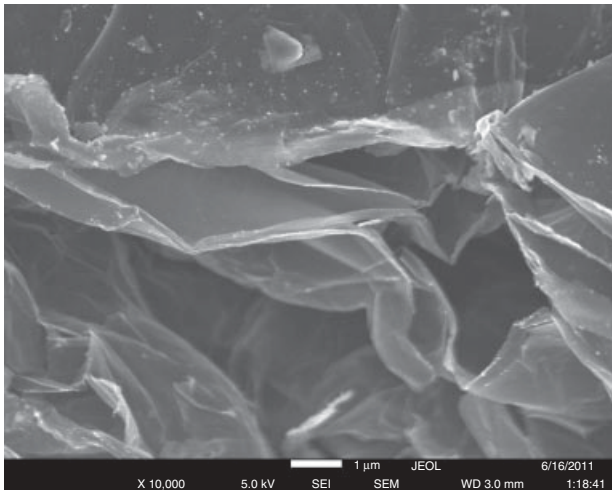

(a)

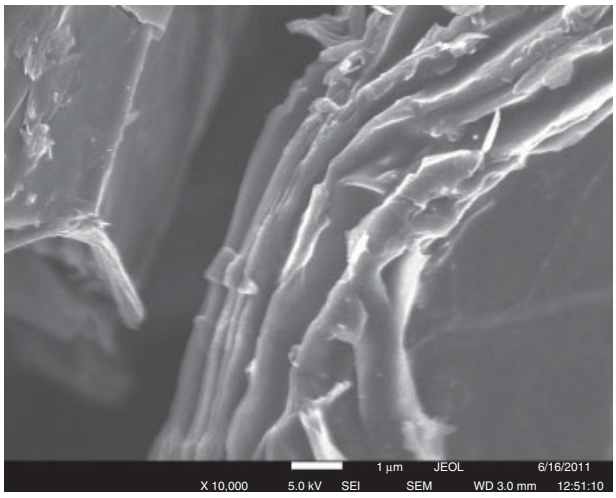

(b)

Figure 31.18 (a) HRSEM micrographs of graphene laminates modified with urea and (b) with L-lysine amino acid.

31.7.2 Surface Modification of Graphene

Pristine graphene materials are unsuitable for intercalation by large species, such as polymer chains, because graphene as a bulk material has a pronounced tendency to agglomerate in a polymer matrix [185]. Considerable work has been carried out on the amination, esterification, isocyanate modification, and polymer wrapping as routes for the functionalization of graphene (Fig. 31.18a and b). The electrochemical modification of graphene using ionic liquids has also been reported.

31.7.3 Polymer/Graphene Nanocomposites

The most important aspect of these nanocomposites is that all these improvements are obtained at very low filler loadings in the polymer matrix. Different types of nanographite forms, such as expanded graphite and exfoliated graphite, have also been used to produce conducting nanocomposites with improved physicochemical properties. Polymer–graphene nanocomposites include those of epoxy [186], PS [187], polyaniline [188], PVA [189], Polyurethane (PU) [190], Polyvinilidene fluoride (PVDF) [191], PET [192], and PC [193] nanocomposites.

31.7.4 Preparation Methods of Polymer/Graphene Nanocomposites

31.7.4.1 In Situ Intercalative Polymerization A variety of polymer nanocomposites have been prepared using this method, that is, PS/graphene, PMMA/expanded graphite, poly(styrene sulfonate) (PSS)/layered double hydroxyl (LDH), PI/LDH, and PET/LDH.

31.7.4.2 Solution Intercalation Graphene or modified graphene can be dispersed easily in a suitable solvent, such as water, acetone, chloroform, tetrahydrofuran (THF), dimethyl formamide (DMF), or toluene, owing to the weak forces that stack the layers together. Polymer nanocomposites based on PE-*g*-MAH/graphite, epoxy/LDH, PS, PP, PVA/graphene, poly(vinyl chloride) (PVC)/carbon nanotubes, ethylene vinyl acetate (EVA)/LDH have been prepared using this method.

31.7.4.3 Melt Intercalation A thermoplastic polymer is mixed mechanically with graphite or graphene or modified graphene at elevated temperatures using conventional methods, such as extrusion and injection molding. A wide range of polymer nanocomposites, such as expanded graphite with HDPE, PPS, and PA6, have been prepared using this method.

31.7.4.4 Dispersion of Graphene into Polymers The improvement in the physicochemical properties of the nanocomposites depends on the distribution of graphene layers in the polymer matrix as well as interfacial bonding between the graphene layers and polymer matrix. Interfacial bonding between graphene and the host polymer dictates the final properties of the graphene-reinforced polymer nanocomposite.

TEM can provide direct images of dispersion and has been widely used to visualize layered silicates in polymers. In addition, rheology can be an effective tool for quantifying nanocomposite dispersion. It averages over many particles and is also useful in its own right for predicting processability. The onset of network formation can be inferred from small strain oscillatory shear versus frequency plots of the storage modulus for a series of concentrations of graphene. The storage modulus becomes independent of frequency at low frequency, a signature of solidlike network formation. The modulus data may

indicate that polymer chains can bridge between particles causing network percolation at a lower concentrations than conductivity percolation.

31.8 CONCLUSIONS

In this chapter, we have reviewed important issues regarding the fundamental and applied research on polymer/clay nanocomposites, including the contributions of our group to the understanding of the properties and behavior of these complex materials. It was not the intention to cover most of the polymer nanocomposite field, rather to expose some of the most important issues and challenges in this area. The last section of this chapter (polymer/graphene systems) shows that this field is fast developing, ensuring a wide research activity and the production of new materials for the future.

ACKNOWLEDGMENTS

We acknowledge the support from UNAM through project PAPIIT IN 116510 and we thank Omar Novelo for the SEM micrographs.

REFERENCES

1. Kojima Y, Usuki A, Kawasumi M, Okada A, Fukushima Y, Karauchi T, Kamigaito O. J Mater Res 1993;8:1185.
2. Okada A, Usuki A. Mater Sci Eng 1995;C3:109.
3. Akkapeddi MK. Polym Comp 2000;21(4):576.
4. Liu L, Qi Z, Zhu X. J Appl Polym Sci 1999;71(7):1133.
5. Cheng LP, Lin DJ, Yang KC. J Memb Sci 2000;172:157.
6. Kawasumi M, Hasegawa N, Kato M, Usuki A, Okada A. Macromolecules 1997;30:6333.
7. Kato M, Usuki A, Okada A. J Appl Polym Sci 1997;66(9): 1781.
8. Heinemann J, Reichert P, Thomann R, Mulhaupt R. Macromol Rapid Commun 1999;20(8):423.
9. Jeong HG, Jung HT, Lee SW, Hudson SD. Polym Bull 1998;41(1):107.
10. Noh MH, Lee DC. J Appl Polym Sci 1999;74(12):2811.
11. Fu X, Qutubuddin S. Polymer 2001;42(2):807.
12. Messersmith PB, Giannelis EP. Chem Mater 1993;5(8):1064.
13. Vaia RA, Vasudevan S, Krawiec W, Scanlon LG, Giannelis EP. Adv Mater (Weinheim) 1995;7(2):154.
14. Levy R, Francis CW. J Colloid Interface Sci 1975;50(3):442.
15. Greenland DJ. J Colloid Sci 1963;18:647.
16. Muzny CD, Butler BD, Hanley HJM, Tsvetkov F, Peiffer DG. Mater Lett 1996;28(4):379.
17. Okamoto M, Morita S, Taguchi H, Kim YH, Kotaka T, Tateyama H. Polymer 2000;41(10):3887.
18. Dietsche F, Mulhaupt R. Polym Bull 1999;43(4–5):395.
19. Ke Y, Long C, Qi Z. J Appl Polym Sci 1999;71(7):1139.
20. Matayabas JC, Turner SR, Sublett BJ, Connell GW, Gilmer JW, Barbee RB, inventors. High I.V. polyester compositions platelet particles. US patent 6084019. 2000.
21. Rosenquist NR, Miller KF, inventors. Composite comprising polymerizes cyclic carbonate oligomer. US patent 4,786,710. 1988.
22. Huang X, Lewis S, Brittain WJ, Vaia RA. Macromolecules 2000;33(6):2000.
23. Giannelis EP. Adv Mater 1996;8(1):29.
24. Aranda P, Ruiz-Hitzky E. Appl Clay Sci 1999;15:119.
25. Usuki A, Koiwai A, Kojima Y, Kawasumi M, Okada A, Kurauchi T, Kamigaito O. J Appl Polym Sci 1995;15:119.
26. Michalczyk MJ, Sharp KG, Stewart CW, inventors. US patent 5,726,247. 1998.
27. Badesha S , Henry A, Maliborski J, Clifford E, inventors. US patent 5,840,796. 1998.
28. Ellsworth MW, inventor. US patent 5,962,553. 1999.
29. Wang M, Pinnavaia T. Chem Mater 1994;6(4):468.
30. Zilg C, Mulhaup R, Finter J. Macromol Chem Phys 1999; 200(3):661.
31. Kornmann X, Berglund LA, Sterte J, Giannelis EP. Polym Eng Sci 1998;38(8):1351.
32. Chen L, Liu K, Yang CZ. Polym Bull 1996;37(3):377.
33. Hirai T, Miyamoto M, Komasawa I. J Mater Chem 1999; 9(6):1217.
34. Wang Z, Pinnavaia TJ. Chem Mater 1998;10(12):3769.
35. Zilg C, Thomann R, Mulhaupt R, Finter J. Adv Mater 1999;11(1):49.
36. Chen TK, Tien YI, Wei KH. J Appl Polym Sci Polym Chem 1999;37(13):2225.
37. Chen TK, Tien YI, Wei KH. Polymer 2000;41(4):1345.
38. Spenleuhauer G, Bazile D, Veillard M, Prud'Homme C, Michalon JP, inventors. US patent 5,766,635. 1998.
39. Biswas M, Sinha Ray S. Polymer 1998;39(25):6423.
40. Sinha Ray S, Biswas M. J Appl Polym Sci 1999;73(14): 2971.
41. Srikhirin T, Moet A, Lando JB. Polym Adv Technol 1998;9(8):491.
42. Tyan H, Liu Y, Wei K. Chem Mater 1999;11(7):1942.
43. Vaia RA, Giannelis EP. Macromolecules 1997;30:7990.
44. Vaia RA, Giannelis EP. Macromolecules 1997;30:8000.
45. Sánchez-Solís A, García-Rejón A, Manero O. Macromol Symp 2003;192:281.
46. Cho JW, Paul DR. Polymer 2001;42:1083.
47. Chung S-C, Hahm W-G, Im S-S, Oh S-G. Macrom Res 2002;10:221.
48. Usuki A, Kawasumi Y, Kojima M, Fukushima Y, Okada A, Kurauchi T, Kamigaito O. J Mater Res 1993;8:1179.
49. Yano K, Usuki A, Okada A, Kurauchi T, Kamigaito O. J Polym Sci A: Polym Chem 1993;31:2493.

50. Yangchuan K, Chenfen L, Zongneng Q. J Appl Polym Sci 1999;71:1139.
51. Krishnamoorti R, Giannelis E. Macromolecules 1997;30: 4097.
52. Rosedale JH, Bates FS. Macromolecules 1990;23:2329.
53. Larson RG, Winey KI, Patel SS, Watanabe H, Bruisma R. Rheol Acta 1993;32:245.
54. Gelfer M, Song HH, Liu L, Avila C, Yang L, Si M, Hsiao BS, Chu B, Rafailovich M, Tsou AH. Polym Eng Sci 1841;2002:42.
55. Schmidt G, Nakatani AI, Butler PD, Han CC. Macromolecules 2002;35:725.
56. Schmidt G, Nakatani AI, Butler PD, Karim A, Han CC. Macromol Commun 2000;33:20.
57. Schmidt G, Nakatani AI, Han CC. Rheol Acta 2002;41:45.
58. Hacket E, Manias E, Giannelis EP. Chem Mater 2000;12: 2161.
59. Krishnamoorti R, Vaia RA, Giannelis EP. Chem Mater 1996;8:1728.
60. Zhang Q, Archer LA. Langmuir 2002;18:10435.
61. Sánchez-Solís A, Romero I, Estrada MR, Calderas F, Manero O. Polym Eng Sci 2004;44:1094.
62. Utracki LA, Lyngaae-Jorgensen J. Rheol Acta 2002;41:394.
63. Stewart ME, Cox AJ, Naylor DM. Polymer 1993;34:4060.
64. Alexandrova L, Cabrera A, Hernández MA, Cruz MJ, Abadie MJM, Manero O, Likhatchev D. Polymer 2002;43: 5397.
65. Kenwright AM, Peace SK, Richards RW, Bunn A, MacDonald WA. Polymer 1999;40:5851.
66. Kyotani M, Pudjiastuti W, Saeed A. J Macromol Sci Phys 1999;38:197.
67. Chen P, Music K, McNeely G, inventors. WO patent 96/35571P. 1996.
68. Tharmapuram SR, Jabarin SA. Adv Polym Technol 2003;22: 137.
69. Sánchez-Solís A, Estrada MR, Cruz J, Manero O. Polym Eng Sci 2000;40:1216.
70. Ito M, Takahashi M, Kanamoto T. Polymer 2002;43:3675.
71. Sánchez-Solís A, García-Rejón A, Martínez-Richa A, Calderas F, Manero O. J Polym Eng 2005;25:553.
72. Sánchez-Solís A, García-Rejón A, Estrada M, Martínez-Richa A, Sánchez G, Manero O. Polym Int 2005;54:1669.
73. Wagener R, Reisinger T. Polymer 2003;44:7513.
74. Krishnamoorti R, Vaia RA, Giannelis EP. Chem Mater 1996;8:1728.
75. Fornes TD, Yoon PJ, Keskkula H, Paul DR. Polymer 2001; 42:9929.
76. Hyun Y, Lim S, Choi S,H, Jhon M. Macromolecules 2001; 34:8084.
77. McAlpine M, Hudson N, Liggat J, Pethrick J, Pugh D, Rhoney I. J Appl Polym Sci 2006;99:2614.
78. Wang Z, Xie G, Wang X, Zhang Z. J Appl Polym Sci 2006;1000:4434.
79. Lertwimolnun W, Vergnes B. Polymer 2005;46:3462.
80. Lertwimolnun W, Vergnes B. Polym Eng Sci 2006;46:314.
81. Letwimolnun W, Vergnes B, Ausias G, Carreau PJ. J Nonnewton Fluid Mech 2007;141:167.
82. Abrányi A, Százdi L, Pukánszky B, Vancsó GJ. Macromol Rapid Commun 2006;27:132.
83. Calderas F, Sánchez-Solís A, Maciel A, Manero O. Macromol Symp 2009;283:354.
84. Mironi-Harpaz I, Narkis M. Polym Eng Sci 2005;45: 174–185.
85. Xu L, Lee J. Polym Eng Sci 2005;45:496.
86. Hasegawa N, Okamoto H, Kato M, Usuki A, Sato N. Polymer 2003;44:2933.
87. Wang K, Wang L, Wu J, Chen L, He C. Langmuir 2005;21: 3613.
88. Wang K, Wu J, Chen L, Toh ML, He C, Yee AF. Macomolecules 2005;38:788.
89. Wang K, Chen L, Kotaki M, Ch H. Compos Appl Sci Manuf 2007;38:192.
90. Bongiovanni R, Mazza D, Roncheti S, Turcato EA. J Colloid Interface Sci 2006;296:515.
91. Rivera-Gonzaga JA, Sanchez-Solis A, Manero O. J Polym Eng 2012:32,1.
92. Bellucci F, Terenzi A, Leuteritz A, Pospiech D, Frache A, Traversa G, Camino G. Polym Adv Technol 2008;19:547.
93. Morawiek J, Pawlak A, Slouf M, Galeski A, Piorkowska E, Krasnikowa N. Eur Polym J 2005;41:1115.
94. Osman M, Rupp J. Macromol Rapid Commun 2005;26:880.
95. Zhou Z, Zhai H, Xu W, Guo H, Liu C, Pan P. J Appl Polym Sci 2006;101:805.
96. Wang K, Choi M, Koo C, Xu M, Chung I, Jang M, Choi S, Song H. J Polym Sci Polym Phys 2002;40:1454.
97. Liang G, Xu J, Bao S, Xu W. J Appl Polym Sci 2004;91: 3974.
98. Wang K, Choi M, Koo C, Choi Y, Chung I. Polymer 2001; 42:9819.
99. Chrissopoulou K, Altintzi I, Anastasiadis S, Giannelis E, Pitsikalis M, Hadjichristidis N, Theophilou N. Polymer 2005;46:12440.
100. Arunvisut S, Phummanee S, Somwangthanaroj A. J Appl Polym Sci 2007;106:2210.
101. Gopakumar T, Kontopoulou M, Parent J. Polymer 2002;43: 5483.
102. Stoeffler K, Lafleur P, Denault J. Polym Eng Sci 2008;48: 2459.
103. Bousmina M. Macromolecules 2006;39:4259.
104. Lee W, Eung S, Hun S, Jin-San Y. J Appl Polym Sci 2005;98:1229.
105. Xie Y, Yu D, Kong J, Fan X, Qiao W. J Appl Polym Sci 2006;100:4004.
106. Walter P, Mader D, Reichert P, Mulhaupt R. J Macromol Sci 1999;A36:1613.
107. Bonilla E, Sanchez-Solís A, Manero O. J Polym Eng 2008;28:553.

108. Hasegawa N, Kawasumi M, Kato M, Usuki A, Okada A. J Appl Polym Sci 1998;67:87.
109. Manias E, Touny A, Wu L, Strawhecker K, Lu B, Chung TC. Chem Mater 2001;13:3516.
110. Ton-That MT, Perrin F, Cole KC, Bureau MN, Denault J. Polym Eng Sci 2004:44, 1212.
111. Kato M, Matsushita M, Fukumori K. Polym Eng Sci 2004;44:1205.
112. Marchant D, Jarayaman K. Ind Eng Chem Res 2002;41: 6402.
113. Okamoto M, Nam PH, Maiti P, Kotaka T, Hasegawa N, Usuki A. Nano Lett 2001;1:295.
114. Svoboda P, Zeng C, Wang H, Lee L, Tomasko D. J Appl Polym Sci 2002;85:1562.
115. Gilman J, Jackson C, Morgan A, Harris R, Manias E, Giannelis E, Wuhenow M, Hilton D, Phillips S. Chem Mater 2000;12:1866.
116. Nalwa H. *Encyclopedia of Nanoscience and Nanotechnology, Polymer-Clay Nanocomposites*. Vol. 8. American Scientific Publishers; 2004. p 823–824.
117. Pinnavaia T, Beall G. *Polymer-Clay Nanocomposites*. London: Wiley; 2000. p 193.
118. Gilman J. Appl Clay Sci 1999;15:31.
119. Zhu J, Wilkie C. Polym Int 2000;49:1158.
120. Porter D, Metcalfe E, Thomas M. Fire Mater 2000;24:45.
121. Gianelli W, Ferrara G, Camino G, Pellegatti G, Rosenthal J, Trombini R. Polymer 2005;46:7037.
122. Ramos L, Melo T, Rabello M, Silva S. Polym Degrad Stab 2005:89,383.
123. Marosi G, Anna P, Marton A, Bertalan G, Bota A, Toth A, Mohai M, Racz I. Polym Adv Technol 2002;13:1103.
124. Morgan A, Harris J, Kashiwagi R, Chyall L, Gilman J. Fire Mater 2002;26:247.
125. Zanetti M, Camino G, Toman R, Mulhaupt R. Polymer 2001;42:4501.
126. Alexandre M, Beyer G, Henrist C, Cloots R, Rulmont A, Jerome R. Macromol Rapid Commun 2001;22:643.
127. Zhang H, Wang Y, Wu Y, Zhang L, Yang J. J Appl Polym Sci 2005;98:844.
128. Costache M, Wang D, Heidecker J, Manias E, Wilkie C. Polym Adv Technol 2006;17:272.
129. Gianelli W, Camino G, Tabuani D, Bortolon V, Savadori T, Monticelli O. Fire Mater 2006;30:333.
130. Wang S, Hu Y, Lin Z, Gui Z, Wang Z, Chen Z, Fan W. Polym Int 2003;52:1045.
131. Wang J, Chow W. J Appl Polym Sci 2005;97:366.
132. Grand A, Wilkie C. Fire Retardancy of Polymeric Materials. M. Dekker: New York (NY), USA. 2000. p 147.
133. Sanchez-Olivares G, Sanchez-Solis A, Manero O. Int J Polym Mater 2008;57:245.
134. Paul DR, Rios-Guerrero L. Polymer 2000;41:542.
135. Donald AM, Kramer EJ. J Appl Polym Sci 1982;27:3729.
136. van Krevelen DW. *Properties of Polymers*. 3rd ed. Elsevier; Amsterdam, The Netherlands. 1990. p 641.
137. Utevski L, Scheinker M, Georlette P, Shoshana L. J Fire Sci 1997;15:375.
138. Song JH. J Vinyl Addit Technol 1995;1:1.
139. Zanetti M, Camino G, Canavese D, Morgan A, Lamelas F, Wilkie C. Chem Mater 2002;14:189.
140. Hu Y, Wang S, Ling Z, Zhuang Y, Chen Z, Fan W. Macromol Mater Eng 2003;288:272.
141. Morgan A. Polym Adv Technol 2006;17:206.
142. Sanchez-Olivares G, Sanchez-Solis A, Manero O. Int J Polym Mater 2008;57:417.
143. Sanchez-Olivares G, Sanchez-Solis A, Camino G, Manero O. Express Polym Lett 2008;2:569.
144. Asai S, Sakata K, Sumita M, Miyasaka K. Polym J 1992;24: 415.
145. Sumita M, Sakata K, Hayakawa Y, Asai S, Miyasaka K, Tanemura M. Colloid Polym Sci 1992;270:134.
146. Gamboa KMN, Ferreira AJB, Camargo SS, Soares BG. Polym Bull 1997;38:95.
147. Tchoudakov R, Breuer O, Narkis M. Polym Eng Sci 1996;36: 1336.
148. Tchoudakov R, Breuer O, Narkis M, Siegmann A. Polym Eng Sci 1928;1997:37.
149. Gubbels F, Blacher S, Vanlathem E, Jerome R, Deltour R, Brouers F, Teyssie P. Macromolecules 1994;28:1559.
150. Soares BG, Gubbels F, Jerome R, Teyssie P, Vanlathem E, Deltour R. Polym Bull 1995;35:223.
151. Sumita M, Alai S, Miyadera N, Jojima E, Miyasaka K. Colloid Polym Sci 1986;264:212.
152. Brewer O, Tchoudakov R, Narkis M, Siegmann A. J Appl Polym Sci 1997;64:1097.
153. Lee B. Polym Eng Sci 1992;32:36.
154. Mallette JG, Marquez A, Manero O. Polym Eng Sci 2000; 40:2272.
155. Foulger SH. J Appl Polym Sci 1899;1999:37.
156. Miyasaka K, Watanabe K, Jojima E, Aida H, Sumita M, Ishkiwa K. J Mater Sci 1982;17:1610.
157. Traugott D, Barlow JW, Paul DR. J Appl Polym Sci 1983; 28:2947.
158. Sambaru P, Jabarin SA. Polym Eng Sci 1993;33:827.
159. Nadkarni VM, Shingankuli VL, Jog JP. J Appl Polym Sci 1992;46:339.
160. Blaszkiewicz M, Mclachlan DS, Newnham RE. Polym Eng Sci 1992;32:421.
161. Mather PJ, Thomas KM. J Mater Sci 1997;32:401.
162. Sichel EK. *Carbon Black–Polymer Composites: The Physics of Electrically Conducting Composites*. Marcel Dekker: New York (NY), USA. 1982.
163. Mallette JG, Quej LM, Marquez A, Manero O. J Appl Polym Sci 2001;81:562.
164. Bala H, Fu W, Guo Y, Zhao J, Jiang Y, Ding X, Yu K, Li M, Wang Z. Colloids Surf 2006;274:71.
165. Fenter P, McBride MT, Srajer G, Sturchio NC, Bosbach D. J Phys Chem B 2001;105:8112.

166. Nagaraja BM, Abimanyu H, Jung KD, Yoo KS. J Colloid Interface Sci 2007;316:645.
167. Nuutinen JP, Clerc C, Törmälä PJ. J Biomater Sci Polym Ed 2003;14:665.
168. Li J, Xu Y, Wu D, Sun Y. Chin Particuol 2003;1:134.
169. Yu S-H, Antonietti M, Cölfen H, Hartmann J. Nano Lett 2003;3:379.
170. Wang T, Cölfen H. Langmuir 2006;22:8975.
171. Wang T, Reinecke A, Cölfen H. Langmuir 2006;22: 8986.
172. Öncül AA, Sundmacher K, Seidel-Morgenstern A, Thévenin D. Chem Eng Sci 2006;61:652.
173. Judat B, Kind MJ. J Colloid Interf Sci 2004;269:341.
174. Qi L, Cölfen H, Antonietti M. Angew Chem Int Ed 2000; 39:604.
175. Qi L, Cölfen H, Antonietti M. Chem Mater 2000;12: 2392.
176. Romero-Ibarra IC, Rodriguez Gattorno G, Garcia Sanchez MF, Sánchez Solís A, Manero O. Langmuir 2010;26: 6954.
177. Garcia NJ, Bazan JC. Clay Miner 2009;44:81.
178. Lee C, Wei X, Kysar JW, Hone J. Science 2008;321: 385.
179. Liu N, Luo F, Wu H, Liu Y, Zhang C, Chen J. J Adv Funct Mater 2008;18:1518.
180. Kelly BT. Carbon 1972;10:429.
181. Bunch JS, Verbridge SS, Alden JS, van der Zande AM, Parpia JM, Craighead HG, McEuen PL. Nano Lett 2008;8: 2458.
182. Steurer P, Wissert R, Thomann R, Muelhaupt R. Macromol Rapid Commun 2009;30:316.
183. Li D, Muller MB, Gilje S, Kaner RB, Wallac GG. Nat Nanotech 2007;3:101.
184. Hummers WS, Offeman RE. J Am Chem Soc 1958;80(6): 1339.
185. Worsley KA, Ramesh P, Mandal SK, Niyogi S, Itkis ME, Haddon RC. Chem Phys Lett 2007;445:51.
186. Wang S, Tambraparni M, Qiu J, Tipton J, Dean D. Macromolecules 2009;42:5251.
187. Stankovich S, Dikin DA, Dommett GHB, Kohlhaas KM, Zimney EJ, Stach EA, Piner RD, Nguyen ST, Ruoff RS. Nature 2006;442:282.
188. Wang DW, Li F, Zhao J, Ren W, Chen ZG, Tan J, Wu ZS, Gentle I, Lu GQ, Cheng HM. ACS Nano 2009;7:1745.
189. Liang J, Huang Y, Zhang L, Wang Y, Ma Y, Guo T, Chen Y. Adv Funct Mater 2009;19:2297.
190. Lee YR, Raghu AV, Jeong HM, Kim BK. Macromol Chem Phys 2009;210:1247.
191. Ansari S, Giannelis EP. J Polym Sci Polym Phys 2009;47: 888.
192. Zhang HB, Zheng WG, Yan Q, Yang Y, Wang J, Lu ZH, Ji GY, Yu ZZ. Polymer 2010;51:1191.
193. Kim H, Macosko CW. Polymer 2009;50:3797.